

## ARTICLE

Received 00th January 20xx,  
Accepted 00th January 20xx

DOI: 10.1039/x0xx00000x

### Supporting Information

#### **High-Throughput Thermal Plasma Synthesis of $\text{Fe}_x\text{Co}_{1-x}$ Nano-Chained Particles with Unusually-High Permeability, and their Electromagnetic Wave Absorption Properties at High Frequency (1-26 GHz)†**

Min-Sun Jang<sup>†a</sup>, Mi Se Chang<sup>†ab</sup>, Young-tae Kwon<sup>a</sup>, Sangsun Yang<sup>a</sup>, Jina Gwak<sup>c</sup>, Suk Jin Kwon<sup>d</sup>, Joonsik Lee<sup>d</sup>, Kyung Song<sup>e</sup>, Chong Rae Park<sup>b</sup>, Sang Bok Lee<sup>d</sup>, Byeongjin Park<sup>†d</sup>, and Jae Won Jeong<sup>†a</sup>

## Video; in-situ TEM

**Fig. S1** Video of in-situ thermal TEM analysis to observe how the morphology of initially-spherical  $\text{Fe}_{0.6}\text{Co}_{0.4}$  particles changed in real time as the temperature increased.

---

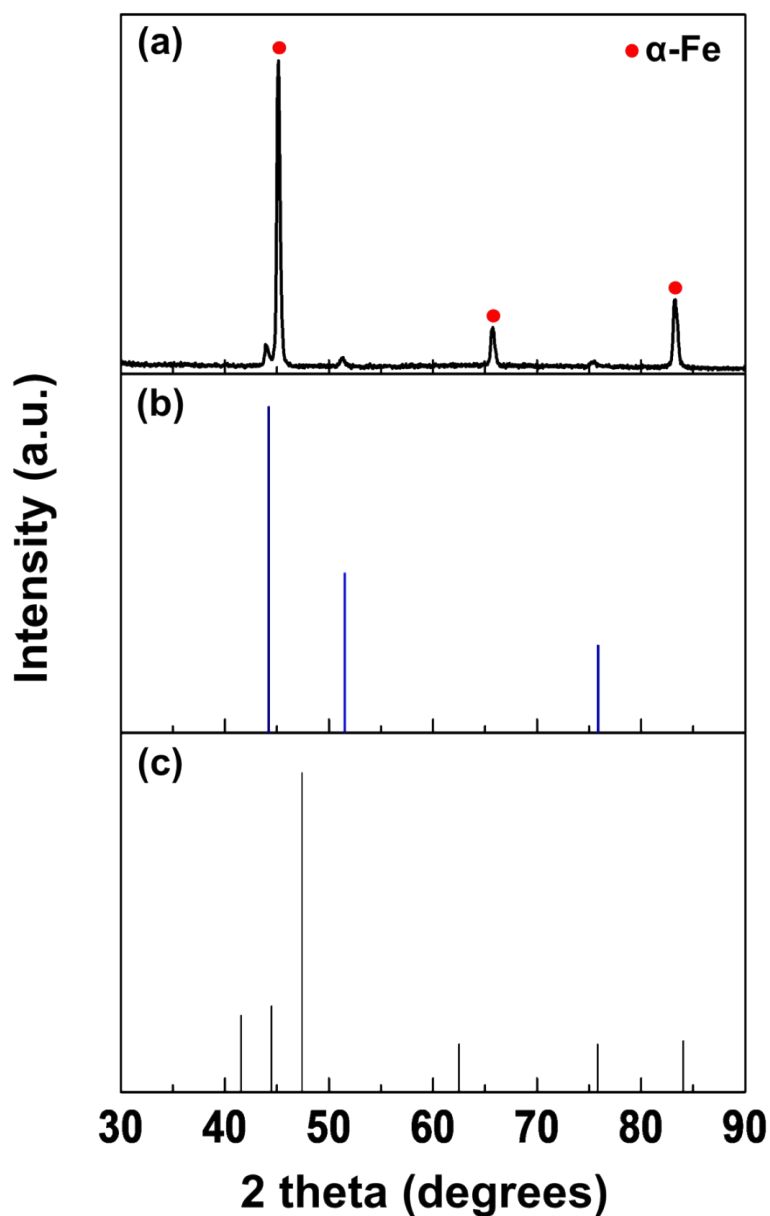


**Fig. S2** (a) Powder X-ray diffraction (XRD) patterns of Fe<sub>0.3</sub>Co<sub>0.7</sub> alloys. All of the prominent peaks, including (110), (200), and (211) planes, correspond to 2θ = 44.8°, 65.2°, and 82.6° those of FeCo with body-centered cubic structure. (b) The relatively low characteristic diffraction peaks at 2θ = 44.2°, 51.5°, and 75.8°, corresponding to Co element with face-centered cubic structures of (111), (200), and (220) planes (PDF # 89-7093). (c) Hexagonal close packed structure of Co element (PDF # 89-7373), which compared with (a), no matching peak was identified.

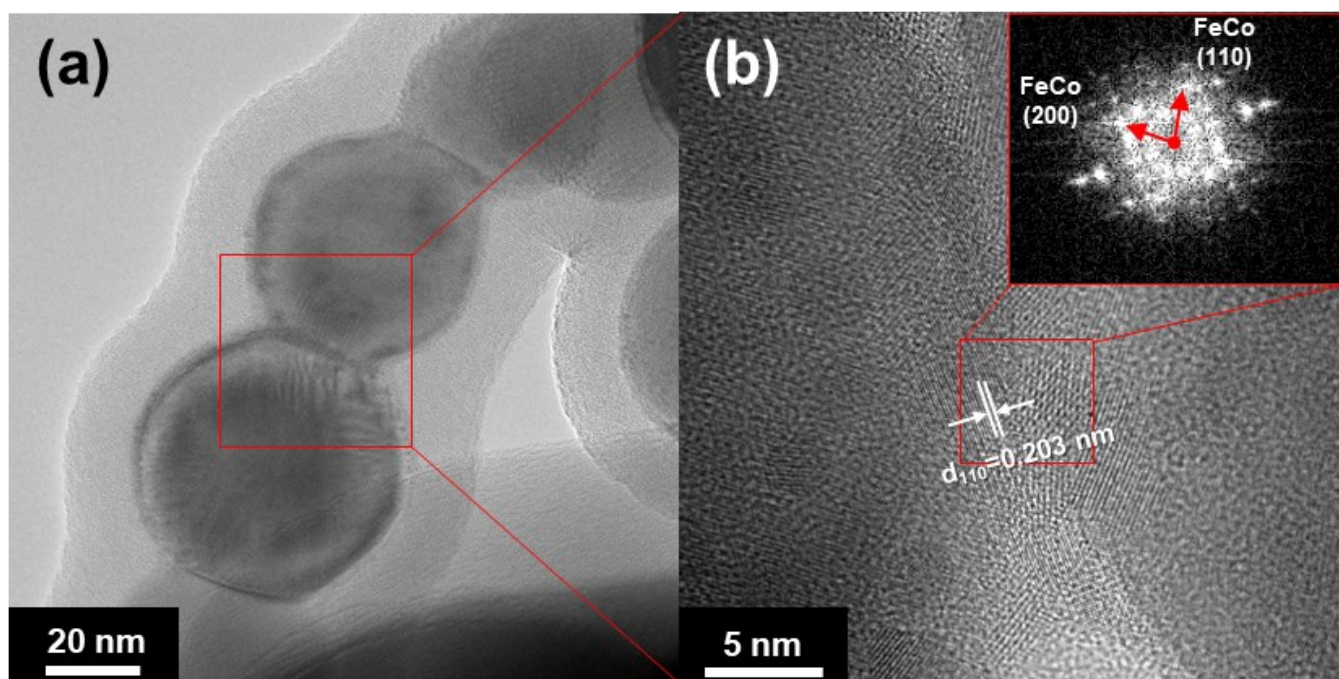


**Fig. S3.** (a) Transmission electron microscope (TEM) images of nano-chained  $\text{Fe}_{0.6}\text{Co}_{0.4}@\text{SiO}_2$  synthesized by the RF-ITP. (b) d-spacing is 0.203 nm on TEM image of the nano-chained  $\text{Fe}_{0.6}\text{Co}_{0.4}@\text{SiO}_2$  with zoomed areas of crystal lattices distances for BCC structure (red).

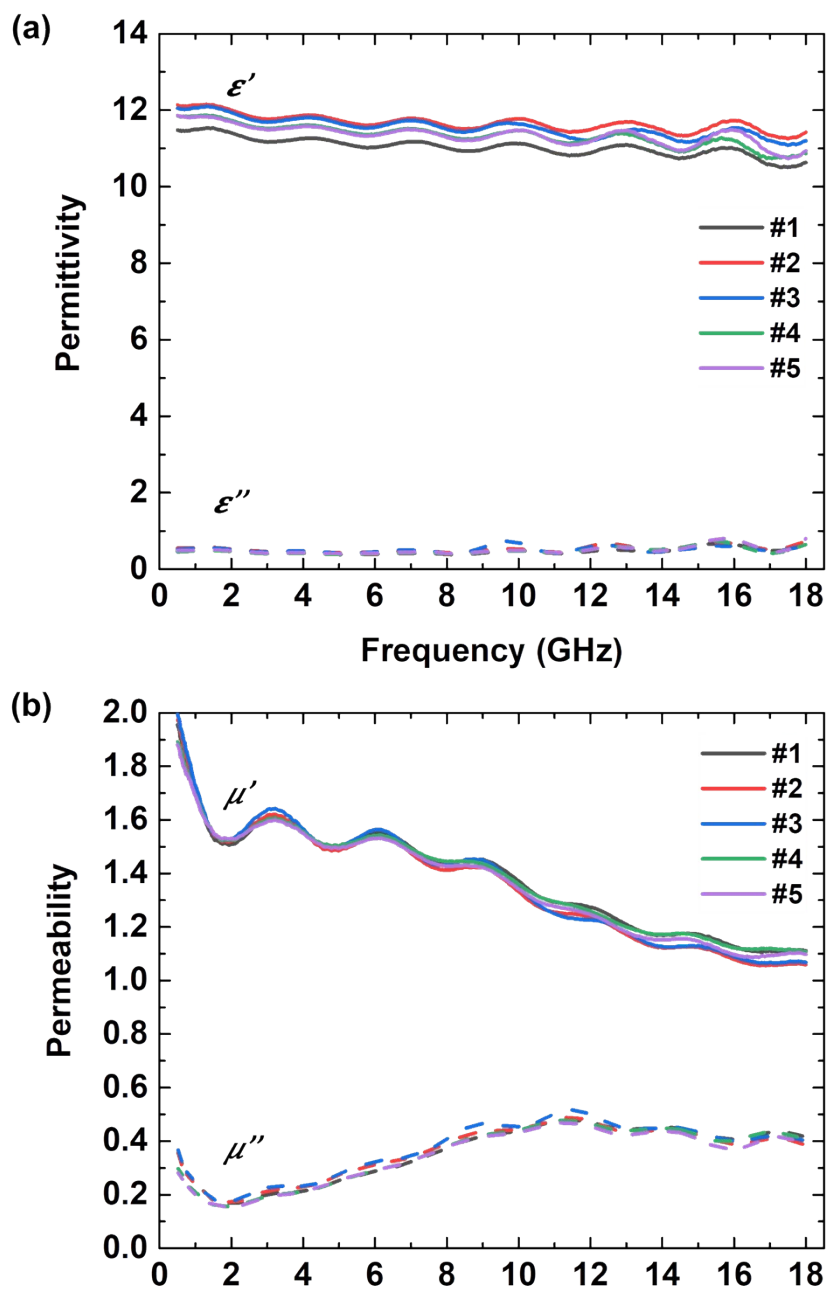


Fig. S4 (a) Complex permittivity and (b) complex permeability comparison result of five different samples. Though the size of each particle in the chain is a little different, it does not seriously affect the electromagnetic properties of the final composite samples.

Though the size of each particle in the chain is a little different, it does not seriously affect the electromagnetic properties of the final composite samples.

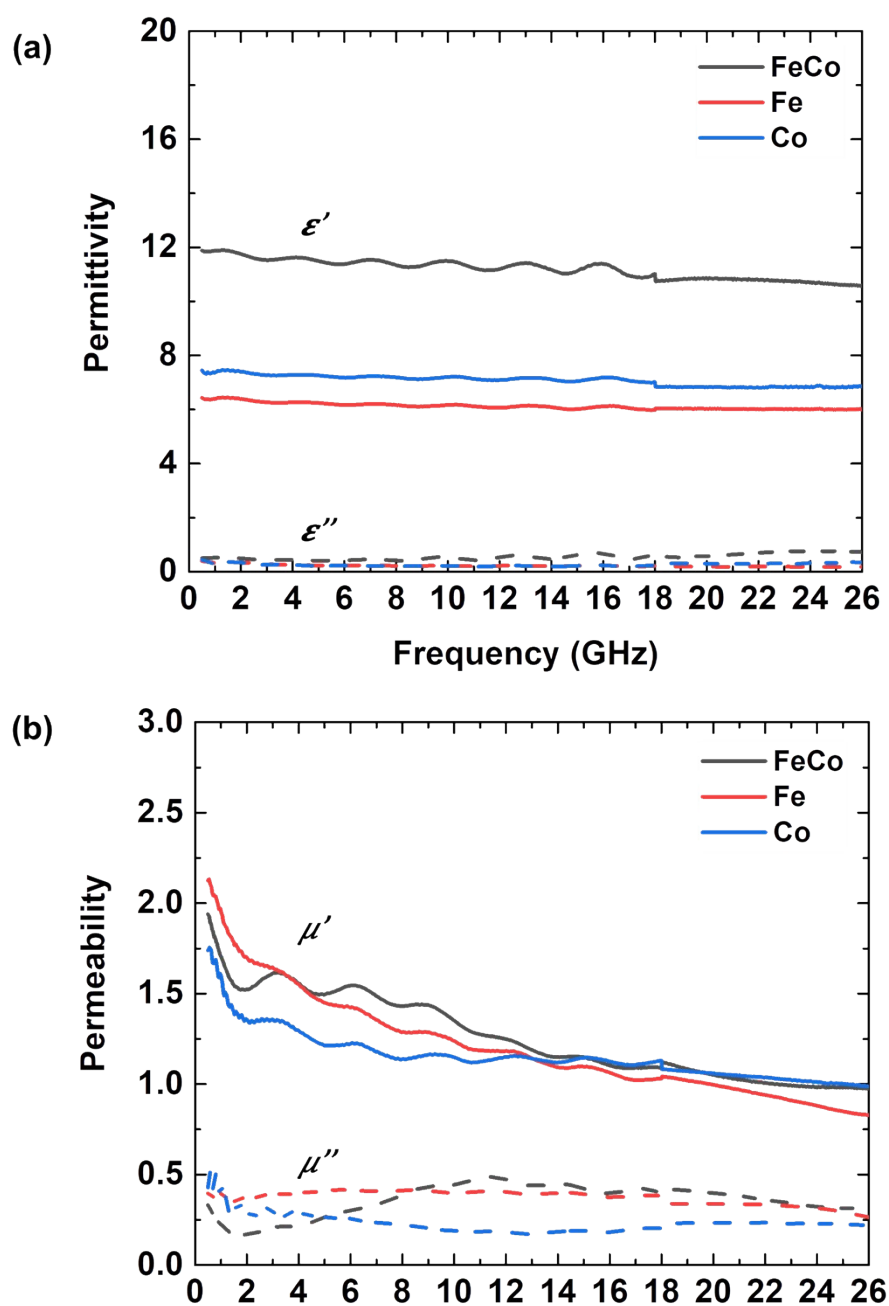


Fig. S5 (a) Complex permittivity and (b) complex permeability comparison result of proposed FeCo nano-chain, Fe nanopowder, and Conanopowder. Pure Fe tends to show high  $\mu''$  while pure Co shows high  $\mu'$ . The proposed FeCo has both high  $\mu'$  and  $\mu''$  in microwave frequency range, which is proper as a high frequency electromagnetic wave absorber.

Pure Fe tends to show high  $\mu''$  while pure Co shows high  $\mu'$ . The proposed FeCo has both high  $\mu'$  and  $\mu''$  in microwave frequency range, which is proper as a high frequency electromagnetic wave absorber.

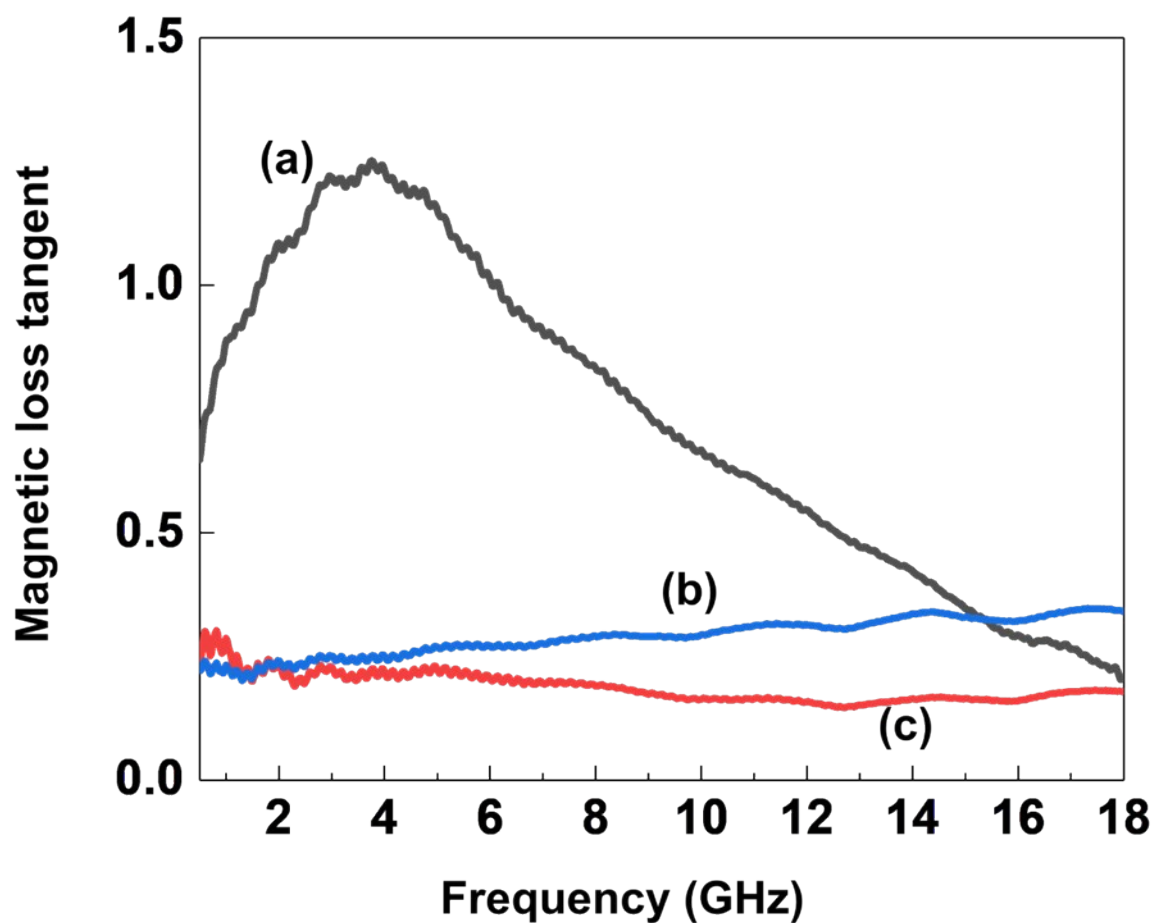


Fig. S6 The frequency dependence of magnetic loss tangent for conventional electromagnetic absorbing materials typically (a) drops dramatically above its resonant frequency (e.g. Sendust), (b) slightly increases at high frequency (e.g. Iron) or (c) decreases as the frequency becomes higher (e.g. Cobalt).

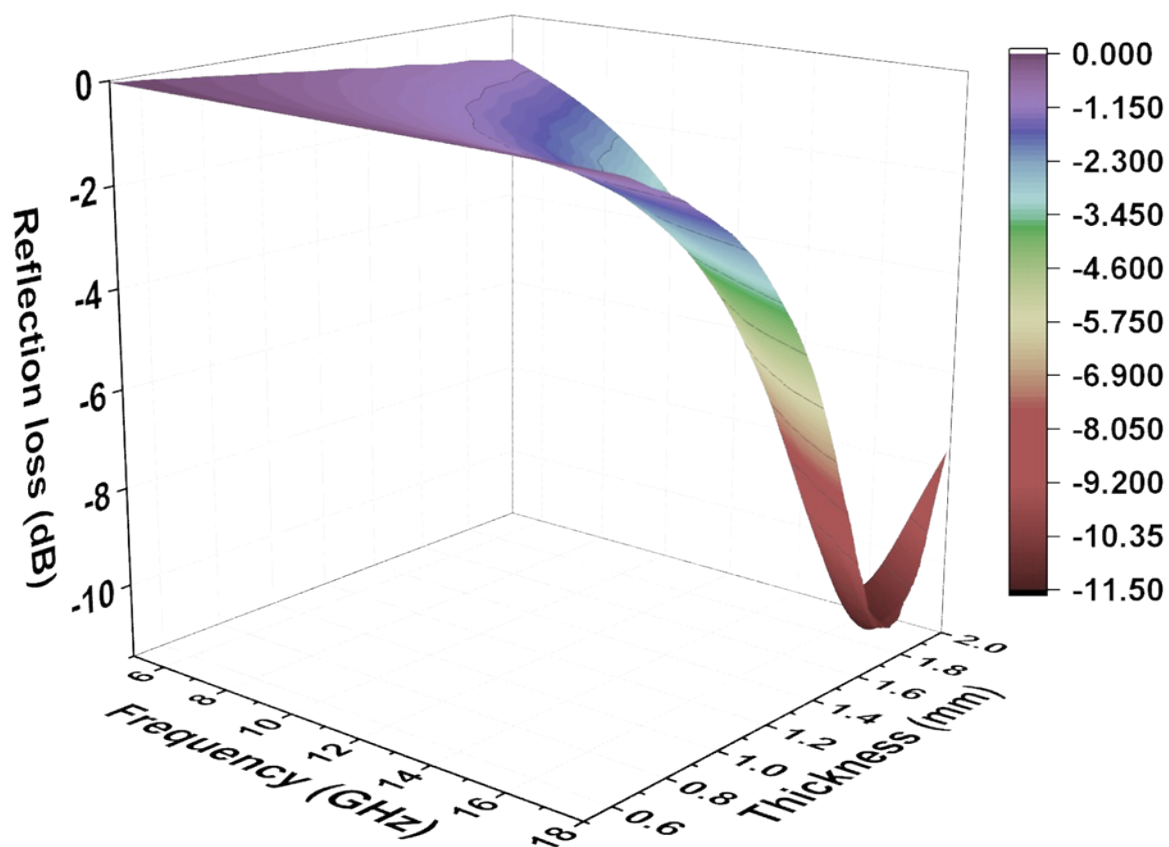


Fig. S7 3-D mapping of overall relationship between reflection loss and frequency (5-18 GHz) of the FeCo spherical micro particles which show only shallow absorption valleys and maximum reflection loss of -11.46 dB at 16.6 GHz.